× 10⁻⁶ mol) and 0.20 mL of the [(C₄H₉)₄N]X solution at 20 °C and monitoring the reaction as a function of time.

Contribution from the Department of Medicinal Chemistry, Hiroshima University School of Medicine, Kasumi, Hiroshima 734, Japan, and Department of Chemistry, College of General Education, Hirosaki University, Bunkyo, Hirosaki 036, Japan

Effects of Imide Anions and Axial Donors on the Stability and Oxidation Behavior of Square-Planar 13–15-Membered Macrocyclic Tetraamine Complexes of Nickel(II) and Copper(II)

EIICHI KIMURA,*[1a] TOHRU KOIKE,[1a] RYOSUKE MACHIDA,[1a] RIEKO NAGAI,[1a] and MUTSUO KODAMA[1b]

Received December 14, 1983

Potentiometric, electrochemical, spectrochemical, and electron spin resonance studies have revealed the structure, stability, and oxidation behavior of square-planar macrocyclic tetraamine complexes of nickel(II) and copper(II) containing a variety of ring sizes (13–15 membered), number (0–3) of imide anions, and extraplanar phenyl, pyridyl, and pyridine N-oxide substituents. Standard electrode potentials $E°$ range from 0.72 to 0.04 V (vs. SCE) for Cu^III,II–macrocycle complexes and from 0.98 to 0.50 V for Ni^III,II–macrocycle complexes in aqueous solutions. The replacement of neutral amine donors of 14-membered tetraamines (N₄) by one to three anionic imide donors successively lowers the $E°$ values by 0.2 V for copper, while the opposite effects were seen for nickel. Oxidation of Ni(II) complexes with an appended pyridyl donor yields five-coordinate Ni(III) species with the neutral N₄ and four-coordinate Ni(III) with the dianionic N₄. Oxidation of the Ni(II) and Cu(II) complexes of N₄ carrying a pyridine N-oxide tail is anomalously facile.

Introduction

The dioxo tetraamines **1**, **8**, and **17**, depicted in Chart I, possess novel ligand properties of saturated macrocyclic tetraamines (N₄) blended with oligopeptide features.[2-6] They accommodate certain metal ions (e.g. Cu²⁺, Ni²⁺, Co²⁺) in the macrocyclic N₄ cavities with simultaneous dissociation of the two amide protons to afford 1:1 complexes generally designated as [M^IIH₋₂L]⁰. Possible resonance stabilization of the resulting imide anions imposes strict N₄ coordinate arrangements for coplanarity, as is the case for tripeptide complexes.[7]

L   square-planar M^IIH₋₂L
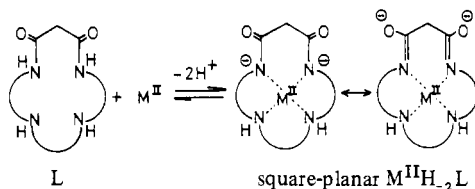
On the other hand, square-planar saturated and unsaturated N₄ ligands have been well demonstrated to stabilize various oxidation states of enclosed Fe,[8] Co,[9,10] or Ni[11,12] in aprotic solvents. The redox properties are determined by various structural parameters: a large ring, the presence of alkyl side chains to interfere with axial solvation, or unsaturation of N donors works for the lower valence states, while absence of these factors or the presence of negative charge on N donors stabilizes higher oxidation states.

Another efficient ligand factor facilitating higher oxidation states of metal ions in aqueous solutions was discovered in oligopeptide complexes of Cu(II)[13] and Ni(II),[14] where anionic imide N donors most dramatically reduce the electrode potentials $E°$ for M^III,II couples, which successively decrease with an increase in the number of deprotonated peptide groups. Hence, highly deprotonated peptide complexes have extremely low potentials (e.g. $E° = 0.30$ V vs. SCE for the quadruply deprotonated N-formyltetraglycine complex of copper CuH₋₄L) such that O₂ oxidation to M(III) may become thermodynamically feasible.[15] It is postulated that oxidative cleavage of peptides by air in the presence of Cu(II) or Ni(II) involves M(III)–peptide complexes as intermediates.

We have been devising simple macrocyclic ligands that produce proper ligand fields and steric environments so as to reproduce certain essential redox functions that occur in natural metal-containing enzymes. Therefore, our recent discovery[4] of the macrocyclic dioxo tetraamines **1**, **8**, and **17** has become highly significant in that they offer a new series of thermodynamically and kinetically efficient prototypes for generation of Cu(III) and Ni(III) in aqueous solutions. We report here the modification and extension of these new dioxo tetraamine structures by varying the number of amide functions and appending extraplanar potential donor functions in order to aim at better catalytic systems and mimic natural systems. Very recently,[5] we reported on novel macrocyclic dioxo pentaamine complexes of high-spin Ni(II) that possess a very low $E°$ value of 0.24 V vs. SCE and can activate O₂ by 1:1 Ni(II)–O₂ complexation so as to oxygenate benzene into phenol at room temperature.[5]

(1) (a) Hiroshima University. (b) Hirosaki University.
(2) Kodama, M.; Kimura, E. *J. Chem. Soc., Dalton Trans.* **1979**, 325.
(3) Kodama, M.; Kimura, E. *J. Chem. Soc., Dalton Trans.* **1979**, 1783.
(4) Kodama, M.; Kimura, E. *J. Chem. Soc., Dalton Trans.* **1981**, 694.
(5) Kimura, E.; Sakonaka, A.; Machida, R.; Kodama, M. *J. Am. Chem. Soc.* **1982**, *104*, 4255.
(6) Machida, R.; Kimura, E.; Kodama, M. *Inorg. Chem.* **1983**, *22*, 2055.
(7) Bossu, F. P.; Margerum, D. W. *J. Am. Chem. Soc.* **1976**, *98*, 4003. The free ligand **8** shows an infrared stretching frequency of the amide carbonyl at 1655 cm⁻¹ (KBr pellet), while its copper(II) complex CuH₋₂L isolable as crystals displays this at 1580 cm⁻¹, supporting the resonance structures for the imide anion complexes.
(8) Herron, N.; Busch, D. H. *J. Am. Chem. Soc.* **1981**, *103*, 1236.
(9) Tait, A. M.; Lovecchio, F. V.; Busch, D. H. *Inorg. Chem.* **1977**, *16*, 2006.
(10) Hung, Y.; Martin, L. Y.; Jackels, S. C.; Tait, A. M.; Busch, D. H. *J. Am. Chem. Soc.* **1977**, *99*, 4029.
(11) Pillsbury, D. G.; Busch, D. H. *J. Am. Chem. Soc.* **1976**, *98*, 7836.
(12) Busch, D. H. *Acc. Chem. Res.* **1978**, *11*, 392.
(13) Bossu, F. P.; Chellappa, K. L.; Margerum, D. W. *J. Am. Chem. Soc.* **1977**, *99*, 2195.
(14) Bossu, F. P.; Margerum, D. W. *Inorg. Chem.* **1977**, *16*, 1210.
(15) Lappin, A. G.; Murray, C. K.; Margerum, D. W. *Inorg. Chem.* **1978**, *17*, 1630.
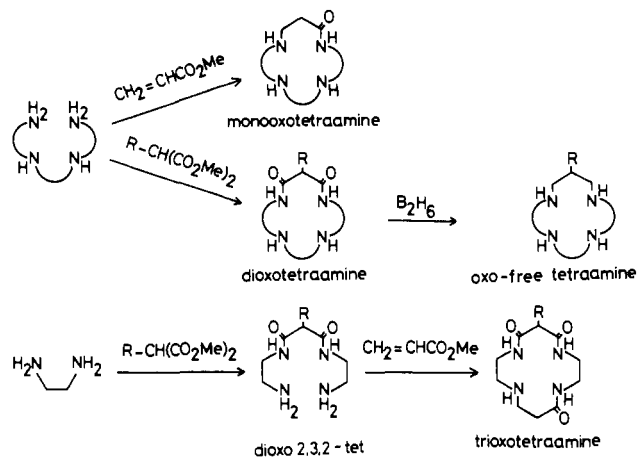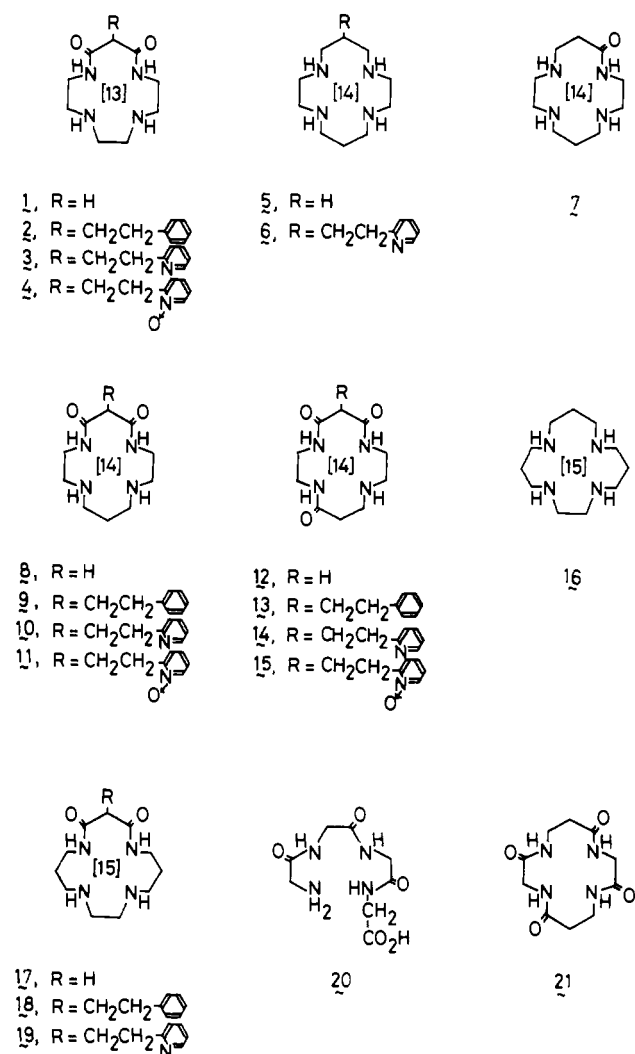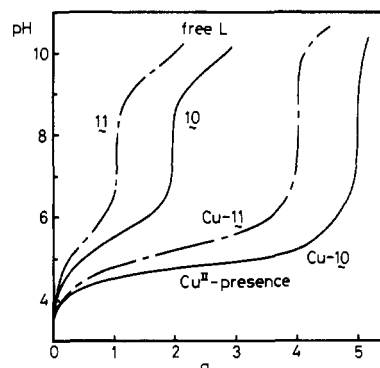
Chart I

1, R = H
2, R = CH₂CH₂⬡
3, R = CH₂CH₂⬡N
4, R = CH₂CH₂⬡N-O

5, R = H
6, R = CH₂CH₂⬡N

7

8, R = H
9, R = CH₂CH₂⬡
10, R = CH₂CH₂⬡N
11, R = CH₂CH₂⬡N-O

12, R = H
13, R = CH₂CH₂⬡
14, R = CH₂CH₂⬡N
15, R = CH₂CH₂⬡N-O

16

17, R = H
18, R = CH₂CH₂⬡
19, R = CH₂CH₂⬡N

20

21

Figure 1. General scheme for the synthesis of macrocyclic tetraamines.

Figure 2. pH titration curves of the pyridyl-substituted tetraamine 10 and pyridine N-oxide substituted 11 (1×10^{-3} M) in the absence and presence of equimolar Cu(II) at 25 °C and $I = 0.2$ M (NaClO₄).

Experimental Section

Materials. The general procedure for preparation of new oxo tetraamine ligands is outlined in Figure 1. Some of the monooxo and dioxo tetraamines[6] were previously reported. The following are representative of preparations of the new dioxo and trioxo tetraamine macrocyclic derivatives.

6-(2-(2-Pyridyl)ethyl)-1,4,8,11-tetraazacyclotetradecane-5,7-dione (10). After a methanol solution (500 mL) of diethyl (2-(2-pyridyl)ethyl)malonate[16] (5.3 g, 20 mmol) and 2,3,2-tet (3,7-diaza-nonane-1,9-diamine, 3.2 g, 20 mmol) was refluxed for 3 weeks, the reaction mixture was concentrated to precipitate a crude product of 10, which was purified by recrystallization from acetonitrile: yield 3.1 g (9.3 mmol); mp 216 °C dec; M⁺ peak m/e 333 (M_r 333.43). Anal. Found (calcd) for C₁₇H₂₇N₅O₂: C, 61.07 (61.24); H, 8.07 (8.16); N, 21.03 (21.00).

6-(2-(2-Pyridyl)ethyl)-1,4,8,11-tetraazacyclotetradecane-5,7,12-trione (14). Diethyl (2-(2-pyridyl)ethyl)malonate (5 g, 19 mmol) was slowly dropped into ethylenediamine (3.4 g, 57 mmol) at room temperature, and stirring was continued until the reaction mixture grew sticky. Then hot methanol was added (250 mL) and the resulting solution was concentrated to ca. 30 mL to precipitate 2.8 g (50%) of 1,9-diamino-5-(2-(2-pyridyl)ethyl)-3,7-diazanonane-4,6-dione (mp 112 °C). Methyl acrylate (830 mg, 9.5 mmol) in 10 mL of methanol was slowly dropped into the refluxing solution of 1,9-diamino-5-(2-(2-pyridyl)ethyl)-3,7-diazanonane-4,6-dione (2.8 g, 9.5 mmol), and the reaction was continued for 24 h. The product 14 was purified by silica gel chromatography (eluent: CHCl₃:CH₃OH:28% aqueous NH₃ = 100:10:1), followed by recrystallization from acetonitrile: yield 1 g (2.9 mmol); mp 240 °C; M⁺ peak m/e 347 (M_r 347.41). Anal.

Found (calcd) for C₁₇H₂₅N₅O₃: C, 58.04 (58.77); H, 7.20 (7.25); N, 19.85 (20.16). The pyridine N-oxide derivatives 4, 11, and 15 were synthesized by treating the pyridyl derivatives 3, 10, and 14 with m-chloroperbenzoic acid. The reaction procedure was as follows in the case of 10. A chloroform solution (30 mL) of the compound 10 (1 g, 3 mmol) and an equimolar amount of m-chloroperbenzoic acid is stirred at 0 °C for 4 h. The solution was washed with 6 N NaOH in order to remove resulting m-chlorobenzoic acid. The chloroform layer was separated and dried with sodium sulfate. The solvent was evaporated, and the crude crystals of 11 were obtained. The product was purified by recrystallization from acetonitrile. A 0.6-g (1.7-mmol) amount of pure 11 was obtained: mp 218 °C dec; M⁺ peak m/e 349 (M_r 349.49). Anal. Found (calcd) for C₁₇H₂₇N₅O₃: C, 58.46 (58.44); H, 7.82 (7.79); N, 20.19 (20.04). The physical data for all of the new compounds are listed in Table I. All of the new ligands are correctly analyzed for C, H, N.

The Cu(II)- and Ni(II)-macrocycle complexes were prepared by combining aqueous solutions of ligand (1.2 equiv) and cupric (nickel) acetate in appropriate neutral to alkaline buffers, where the complexation is complete, as determined from pH titration data. We confirmed the excess ligands neither interfere in nor change the electrochemical, spectroscopic, and ESR measurements.

Apparatus and Measurements. Potentiometric titrations and data analysis for monooxo[6] and dioxo tetraamine complexes[4] were conducted in the same ways as the previous ones. For analysis of pyridyl-ethyl-substituted dioxo tetraamines (see Figure 2) and trioxo tetraamines (Figure 3), the details are described in the supplementary material. The complex stoichiometries and complexation constants thus determined are summarized in Table II.

Cyclic voltammetry was used to determine the electrode potentials $E°$ of a series of the present M(II)-macrocycle complexes in a similar fashion as before[4] or as those applied on peptide complexes of Cu(II)[13] and Ni(II).[14] The electrodes used were glassy carbon (working electrode), platinum wire (auxiliary electrode), and saturated calomel (reference electrode). Typical voltammograms were obtained in Na₂SO₄ (0.5 M) solution at 25 ± 0.05 °C and a scan rate of 100 mV s⁻¹ for metal complexes (2×10^{-3} M). The $E°$ values were obtained

(16) Boekelheide, V.; Rothchild, S. *J. Am. Chem. Soc.* **1947**, *69*, 3149.

Table I. Various Properties of New Macrocyclic Polyamines

macrocyclic polyamine	mp, °C	^{1}H NMR,^{a} δ			protonation constants^d		
		-CONH-	-NH-CH_2-	Ar H	log K_1	log K_2	log K_3
1^b	188–189	...	8 H, 2.6–2.8		9.05	3.82	
2	215–216	2 H, 7.4–7.7	8 H, 2.4–2.8	5 H, 7.0–7.3	9.11	3.79	
3	214–217	2 H, 6.8–7.1	8 H, 2.6–2.8	4 H, 7.0–7.2 (m), 7.5–7.7 (p), 8.4–8.6 (o)	9.09	5.57	3.89
4^b	~222 dec	...	8 H, 2.5–2.8	4 H, 7.1–7.3 (m), 7.6–7.8 (p), 8.4–8.6 (o)	8.78	5.28	
5	198–199		16 H, 2.7–2.9		11.50	10.30	
6	5HCl salt		16 H, 2.5–3.0	4 H, 7.0–7.2 (m), 7.5–7.7 (p), 8.4–8.6 (o)	11.55	10.42	5.32
7	150–151	1 H, 8.7–9.1	12 H, 2.6–3.0		10.42	7.11	3.2
8	174–175	2 H, 7.2–7.6	8 H, 2.6–2.9		9.57	5.97	
9	217–218	2 H, 7.1–7.8	8 H, 2.4–2.8	5 H, 7.1–7.3	9.69	5.81	
10^b	216–217	...	8 H, 2.5–2.8	4 H, 7.0–7.3 (m), 7.5–7.8 (p), 8.4–8.5 (o)	9.70	6.01	4.19
11^c	~218 dec	...	8 H, 2.5–2.8	4 H, 7.1–7.4 (m), 7.6–7.9 (p), 8.4–8.5 (o)	9.45	5.34	
12^b	160–161	...	4 H, 2.6–2.9		8.38		
13^b	239–241	...	4 H, 2.5–2.9	5 H, 7.1–7.3	7.71		
14^b	235–236	...	4 H, 2.6–2.9	4 H, 7.2–7.4 (m), 7.6–7.9 (p), 8.4–8.5 (o)	7.70	5.05	
15^b	~193 dec	...	4 H, 2.6–2.9	4 H, 7.1–7.4 (m), 7.6–7.8 (p), 8.4–8.5 (o)	5.43		
18	203–205	2 H, 7.3–7.6	8 H, 2.5–2.8	5 H, 7.1–7.3	9.39	6.33	
19	196–197	2 H, 7.9–8.1	8 H, 2.6–2.9	4 H, 7.0–7.3 (m), 7.5–7.8 (p), 8.4–8.6 (o)	9.44	6.45	5.35

^{a} All NMR samples run in $CDCl_3$ with Me_4Si internal standard unless otherwise specified. ^{b} NMR samples run in $CDCl_3/CD_3OD$. ^{c} NMR samples run in CD_3OD. ^{d} At 25 °C. I = 0.2 M ($NaClO_4$).
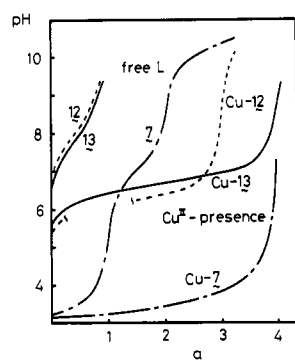

Figure 3. pH titration curves of oxo tetraamine 7, unsubstituted trioxo tetraamine 12, and phenethyltrioxo tetraamine 13 (1 × 10^{-3} M) in the absence and presence of equimolar Cu(II) at 25 °C and I = 0.2 M ($NaClO_4$).

from an average of three independent solution measurements and have a reproducibility of ±3 mV. As a supporting electrolyte, we have consistently used 0.5 M sodium sulfate. The variation of sulfate concentration (0.1–1 M) and displacement of Na_2SO_4 for $NaClO_4$ (0.1–0.5 M) generally increased irreversibility of the cyclic voltammograms but did not significantly alter $E°$ values of Cu(II)– and Ni(II)–macrocyclic polyamine complexes except for Ni(II)–5, where sulfate strongly stabilized Ni(III)–5 by axial coordination.[17] The separation of the anodic and cathodic peaks was 60–90 mV in all but a few cases (~120 mV for Ni–4 (11)), and peak current ratios were near unity. These features are indicative of quasi-reversible electrochemical behavior and, therefore, the midpoint between the oxidation peak and the reduction peak was taken as the electrode potential $E°$ for $M^{II,III}$ couples. All of the $E°$ values thus obtained are summarized in Table II.

The ESR spectra were recorded on a JES-FE1X spectrometer operating at 9300 MHz and equipped with a dual cavity. A small sample of Mn^{2+} was placed in the reference cavity. Two spectra were recorded for each sample, the field being swept in opposite directions and the average of the g values taken. The g values were calculated by the approximation method of Knenbühl.[18] The $g_{\parallel}$ values are accurate to ±0.05 and the $g_{\perp}$ values to ±0.01. The sample tube was placed in a small Dewar flask filled with liquid N_2 and designed so that it would fit in the sample cavity of the ESR spectrometer.

Results and Discussion

Copper(II) and Nickel(II) Complexes. The typical pH titration curves for substituted dioxo tetraamines in the presence
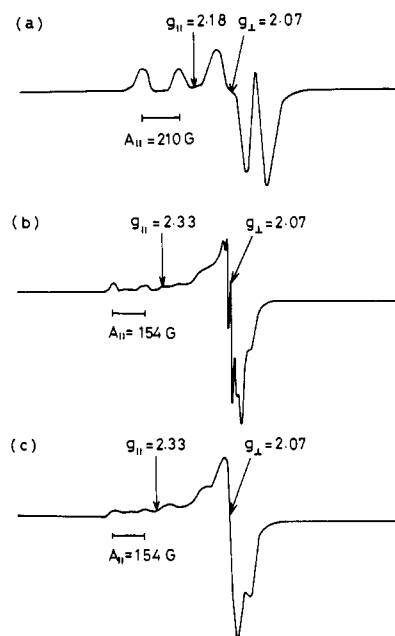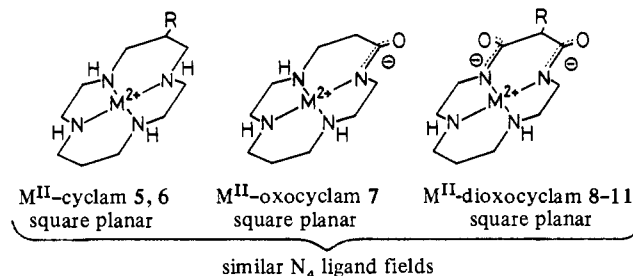
(17) Zeigerson, E.; Ginzburg, G.; Meyerstein, D.; Kirschenbaum, L. J. *J. Chem. Soc., Dalton Trans.* **1980**, 1243.
(18) Knenbühl, *J. Chem. Phys.* **1960**, *33*, 1074.

Figure 4. X-Band ESR spectra of the Cu(II)–singly deprotonated 7 complex (a) and the Cu(II)–doubly deprotonated 12 complex in H_2O (b) and in D_2O (c) at 77 K.

of copper(II) ion (Figure 2) show deprotonation of the two amides for complexation. Accordingly, the complexation constants K_{MH_2L} were calculated in a fashion similar to those for unsubstituted dioxo tetraamine cases,[2] except for the pyridyl-substituted complexes. The dissociation of an amide proton from oxocyclam 7 at pH >4 to sequester M(II) is

M^{II}–cyclam 5, 6
square planar

M^{II}–oxocyclam 7
square planar

M^{II}–dioxocyclam 8–11
square planar

similar N_4 ligand fields

similarly demonstrated by the pH titration curve (Figure 3). Of the same 14-membered macrocyclic frame of the oxo-free (5), monooxo (7), and dioxo tetraamines (8), the visible absorption spectra (for Cu(II) complexes, λ_{max} 505–510 nm; for

Table II. Stability Constants, Visible Absorption Maxima, and Redox Potentials (for M(II) $\rightleftarrows$ M(III)) of Cu(II)- and Ni(II)-Macrocyclic Polyamine Complexes
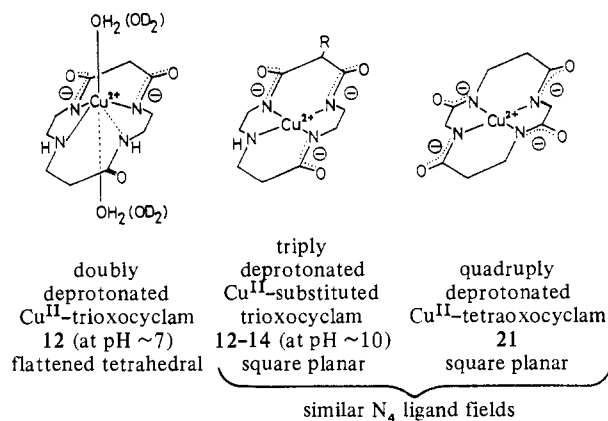
	Cu(II) complexes			Ni(II) complexes		
	log $K_{CuH_{-2}L}$,[a] M	λ_{max},[b] nm (ϵ, M^{-1} cm^{-1})	$E°$,[c] V vs. SCE	log $K_{NiH_{-2}L}$,[a] M	λ_{max}, nm (ϵ, M^{-1} cm^{-1})	$E°$, V vs. SCE
1	−2.22	520 (100)	0.56 (pH 8.5–10.0)	−6.05	412 (110)	0.90 (pH 9.0–10.0)
2	−3.66	520 (105)	0.58 (pH 9.0–10.5)	−6.50	414 (80)	0.98 (pH 9.5–10.5)
3	−3.34	527 (110)	0.56 (pH 9.0–10.5)	−7.11	417 (85)	0.90 (pH 9.5–10.5)
4	−6.21	522 (120)[e]	irrev (pH 7.0)[e]	−9.15	420 (100)[e]	irrev (pH 8.0)[e]
		479 (280)[f]	0.04 (pH 11.7–12.0)[f]		423 (260)[f]	0.63 (pH 11.6–12.0)[f]
5		506 (80)	irrev		450 (70)	0.50 (pH 3.1–7.0)
6		510 (105)	irrev		455 (55)	0.50 (pH 3.5–7.0)
7	(13.00)[d]	510 (80)	0.86 (pH 3.5–8.0)	(4.00)[d]	448 (60)	irrev
8	1.00	505 (100)	0.64 (pH 7.5–10.0)	−5.15	460 (100)	0.81 (pH 8.3–10.0)
9	−1.10	502 (95)	0.66 (pH 9.5–10.0)	−6.30	455 (70)	0.88 (pH 9.0–10.0)
10	−1.00	507 (100)	0.66 (pH 9.2–10.0)	−5.94	457 (80)	0.86 (pH 9.0–10.0)
11	−2.34	512 (100)[e]	irrev (pH 7.0)[e]	−10.25	448 (90)[e]	irrev (pH 8.0)[e]
		481 (240)[f]	0.20 (pH 11.9–12.2)[f]		443 (120)[f]	0.50 (pH 11.9–12.2)[f]
12	−9.24	620 (130)[e]	0.43 (pH 12.5)[f]		no complexation	
13	(−16.34)[g]	490 (80)[f]	0.49 (pH 8.0–9.5)		no complexation	
14	(−16.20)[g]	490 (80)[f]	0.49 (pH 8.0–9.8)		no complexation	
15	(ca. −18)[g]	440 (sh)	0.09 (pH 12.3)		no complexation	
16		575 (150)	irrev		560 (10)	0.77 (pH 4.5–7.0)
17	−4.49	520 (100)	0.69 (pH 9.0–10.0)	−8.92	450 (100)	0.62 (pH 9.0–10.0)
18	−4.43	510 (90)	0.72 (pH 9.5–10.0)	−8.65	451 (90)	0.62 (pH 9.0–10.0)
19	−4.23	510 (95)	0.69 (pH 9.5–10.0)	−8.94	450 (90)	irrev
20		520 (145)	0.38 (pH 10.0)			
21		488 (54)	0.23 (pH 12.0)			

[a] Cumulative formation constants $K_{MH_{-2}L}$ ($=[MH_{-2}L][H^+]^2/[M][L]$) with confidence limits of ±0.05 at I = 0.2 M (NaClO$_4$) and 25 °C (35 °C for Ni) unless otherwise listed.   [b] Visible absorption maximum of the doubly deprotonated metal(II) complex unless otherwise noted.   [c] Redox potentials for M(II) $\rightleftarrows$ M(III) couples, reproducible within ±0.005 V in the pH range specified in parentheses. The values were taken from the midpoint between the oxidation and the reduction peaks in the cyclic voltammograms at 50–200 mV s^{-1} with a glassy-carbon electrode, 25 °C, in 0.5 M Na$_2$SO$_4$.   [d] log $K_{MH_{-1}L}$ ($=$log $[MH_{-1}L][H^+]/[M][L]$).   [e] At pH 7 (pH 8 for Ni) for the species corresponding to MH$_{-2}$L.   [f] At pH 12 for the species corresponding to MH$_{-3}$L (see the text).   [g] log $K_{MH_{-3}L}$ ($=$log $[MH_{-3}L][H^+]^3/[M][L]$) in units of M^2.

Ni(II), λ_{max} 450–460 nm) and ESR spectra (for paramagnetic Cu(II) complexes, see Figure 4a), respectively, are nearly the same, indicating more or less the same macrocyclic square-planar N$_4$ ligand fields. The aqueous solution magnetic measurement by the Evans method[19] showed that Cu(II) and Ni(II) complexes with **6, 7,** and **8–11** are all paramagnetic (S = $^1/_2$, μ_{eff} = 1.64–1.80 μ_B at 35 °C) and diamagnetic (μ $\approx$ 0 at 35 °C), respectively. However, the Ni^{II}–**5** complex (in aqueous solution at pH 9.5) is exceptionally a mixture of low spin and high spin (μ_{eff} = 1.88 μ_B at 35 °C), implying involvement of appreciable axial H$_2$O coordination.

The pH titration data for trioxocyclam **12** (Figure 3) shows the dissociation of only two amide protons at the buffer region pH ~6 in the presence of Cu(II) for the doubly deprotonated complex CuH$_{-2}$L (log $K_{CuH_{-2}L}$ = −9.24) with the third amide hydrogen remaining undissociated. Since the undissociated

doubly deprotonated Cu^{II}-trioxocyclam **12** (at pH ~7) flattened tetrahedral	triply deprotonated Cu^{II}-substituted trioxocyclam **12–14** (at pH ~10) square planar	quadruply deprotonated Cu^{II}-tetraoxocyclam **21** square planar

similar N$_4$ ligand fields

amide N would not interact with Cu(II) as strongly as the other three N donors, square-planar geometries adopted by

other macrocyclic N$_4$ complexes cannot be achieved. The CuH$_{-2}$L part of **12** is blue (λ_{max} 620 nm), greatly differing from the pink (λ_{max} 505–510 nm) shown by oxo-free to dioxo tetraamine homologues. The much higher d–d absorption band and smaller $A_{\parallel}$ ESR parameters ($=$154 G, Figure 4b) for the doubly deprotonated trioxocyclam than those for the other tetraamines (e.g. $A_{\parallel}$ = 210 G for **8**, Figure 4a) imply a distorted complex structure such as a flattened tetrahedron for the former complex, where Cu(II) lies above the N$_4$ cavity. Two axial H$_2$O groups, which are deduced from the disappearance of superhyperfine structures along the z axis in D$_2$O solution (Figure 4c),[20] may assist stabilizing such an incomplete complex structure. At higher pH (12–14) the blue solution of **12** turns to violet, for which the spectrophotometric titration data support the dissociation of the third amide proton with its dissociation constant K ($=[CuH_{-3}L][H^+]/[CuH_{-2}L]$) $\approx$ 10^{-10} M.

In this connnection it is of significance that the dissociation of all of the three amide protons (to CuH$_{-3}$L) simultaneously occurs at pH 7–8 with trioxocyclams **13** (see Figure 3) and **14** possessing the side arm of an aromatic group, whereupon copper(II) ion will go into the macrocyclic N$_4$ cavity. This structure is identified by the visible (λ_{max} 490 nm) and ESR spectra of CuH$_{-3}$L complexes similar to those for the above mentioned square-planar N$_4$ complexes, e.g. **5, 7,** and **8–10.** The hydrophobic aromatic groups may help increase the acidity of the amide hydrogens so as to render their complete dissociation much easier. It ought to be recalled that tetraoxocyclam **21** yields a quadruply deprotonated amide complex CuH$_{-4}$L only at very alkaline conditions, pH >13.[21,22] The

(19) Evans, D. F. *J. Chem. Soc.* **1959**, 2003.

(20) The superhyperfine splittings remarkably strengthen at higher pH (10–11, borate–NaOH buffer), which may indicate OH⁻ (rather than H$_2$O) axial coordination. The reasons for appreciably large proton couplings are not understood.

(21) Rybka, J. S.; Margerum, D. W. *Inorg. Chem.* **1980**, *19*, 3068.

(22) Rybka, J. S.; Margerum, D. W. *Inorg. Chem.* **1981**, *20*, 1453.

visible absorption spectrum of CuH$_{-4}$L with 21 (λ_{max} 488 nm, ϵ 54 M^{-1} cm^{-1}) is very similar to that for the above triply deprotonated trioxocyclam 13 (λ_{max} 490 nm, ϵ 80 M^{-1} cm^{-1}). The lowest wavelength among the present 14-membered tetraamine copper(II) family indicates the most severe tightness of the macrocyclic cavity, which causes the strongest metal–nitrogen interaction over those in oxo-fre (λ_{max} 506 nm), monooxo (510 nm), or dioxo homologues (505 nm). Nickel(II) ion fails to form complexes with any of the trioxocyclam ligands at measurable pH, indicating that these macrocyclic ligands can hardly accommodate Ni(II) due to the insufficient Ni–N bond strength to compensate for the dissociation of the three amide hydrogens.

The anticipated axial coordination of the ethylene-bridging pyridyl N in the 13–15-membered dioxo tetraamine complexes of M(II) with 3, 10, and 19 is hardly recognizable in light of the similarities in values of $K_{MH_{-2}L}$ and visible spectra (and ESR spectra for Cu(II)) with those for phenyl-substituted homologues 2, 9, and 18. This is also the case for the oxo-free tetraamine 6.[23] It is concluded, therefore, that the possible tightness of N$_4$ cavities by the macrocyclic frame would cause extreme elongation of axial bondings. The unperturbed square-planar ligand fields of the macrocyclic N$_4$ ligands are also illustrated by the fact that the attachment of side-arm donors such as pyridyl and primary amine[24] does not alter the (yellow) low-spin d^8 state ($\mu_{eff} \approx 0$) of the Ni(II) complexes. It is of interest to point out that the inclusion of these extra N donors within the macrocyclic frame yields (pink) high-spin Ni(II) complexes.[5]

The pyridyl group, rather, contributes to the net destabilization of the complexes (see $K_{MH_{-2}L}$ values in Table II), whose magnitude tends to vary with the macrocyclic ring size. In the complex of 14-membered 10 with Cu(II) it exerts the greatest destabilization effect. However, for the larger and more flexible 15-membered homologue 19, it has almost no effect. A parallel trend with the ring size is evident in Ni(II) complexes. In the complex of 13-membered 3 having the greatest Ni–N interaction, as demonstrated by the highest d–d energy, the pyridyl group most significantly destablizes the complex. As the ring size is larger, the destabilizing effect becomes smaller. The phenyl group in 2, 9, and 18 brings about almost the same degree of the destabilizing effects as the pyridyl, which suggests that the sole steric factor of phenyl and pyridyl is responsible for the complex destabilization. These aromatic rings would effectively block the axial hydration.

The incorporation of a pyridine N-oxide (py→O) substituent in complexes of 4 and 11 is of special interest. (The pyridine N-oxidation failed for dioxo-free 6 and the 15-membered dioxo compound 19.) It affects Cu(II) complex formulas, and it exerts a greater destabilization effect than any other substituent. Below pH 10 the normal dissociation of the two amide protons occurs to yield CuH$_{-2}$L (see a titration curve in Figure 2), which display visible spectra similar to those for dioxo tetraamine homologues (see Table II). However, at higher pH (11–12) the aqueous solution turns from pink to red (e.g. λ_{max} 522 → 479 nm for 4), indicating certain structural changes of the copper complexes. Such a change is not observed for pyridine and phenyl substituents up to pH $\sim$13. The spectrophotometric titrations established the deprotonation equilibrium expressed by eq 1, where the depro-

$$[CuH_{-2}L]^0 \rightleftharpoons [CuH_{-3}L]^- + H^+$$
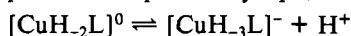
$$K = [CuH_{-3}L][H^+]/[CuH_{-2}L] \qquad (1)$$

tonation constants K are determined to be 2.5 × 10^{-11} M (for

4) and 1.0 × 10^{-11} M (for 11). Incidentally or not, these values are similar to the deprotonation constant ($\sim$10^{-10} M) for CuH$_{-2}$L $\rightleftharpoons$ CuH$_{-3}$L + H$^+$ with trioxocyclam 12. The third deprotonation may occur from the secondary amine of the macrocycles. It is to be noted that the visible absorptions
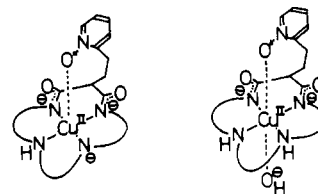
two possible structures for triply deprotonated Cu^{II}–4 and 11

occur almost at the same wavelengths for the triply deprotonated trioxocyclams. The facile dissociation of the third proton is probably due to the axial π interaction of the pyridine N-oxide that can exert an electron-withdrawing effect on the equatorial ligand. The third deprotonation may also be interpreted as arising from the axial OH coordination. The Cu(II)–N-oxide complexes are all shown to be paramagnetic ($S = {}^1/_2$) by the Evans method. The ESR spectra of the Cu^{II}–11 complex at neutral and alkaline pH, unlike those of other Cu(II)–dioxo tetraamine complexes, show perturbed, unresolvable absorptions, implying certain interaction of the N-oxide donor with the copper(II) ion.

Nickel(II) similarly yields the doubly deprotonated Ni^{II}H$_{-2}$L at neutral pH and the triply deprotonated Ni^{II}H$_{-3}$L complexes with 4 and 11 at alkaline pH: the third deprotonation constants for eq 1 were determined potentiometrically to be $\sim$3 × 10^{-10} M (for 4) and <10^{-11} M (for 11). The strong back-bond effect of the pyridine N-oxide donor in Ni^{II}H$_{-2}$L is indicated by the appreciable upfield shift of the pyridine ring hydrogens C$_2$-H, C$_3$-H, and C$_4$-H, as compared to those for free L.
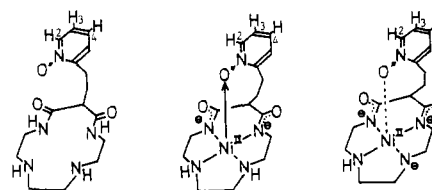
	L (=4) (at pD 7–12)	Ni^{II}H$_{-2}$L (at pD 7)	Ni^{II}H$_{-3}$L (at pD 12)
δ(C$_3$-H)	7.26–7.45	6.80–7.08	7.20–7.70
δ(C$_4$-H)	7.72–7.95	7.28–7.55	7.70–8.00
δ(C$_2$-H)	8.40–8.53	7.90–8.15	8.30–8.60

Me$_4$Si external standard

These protons are subject to downfield shift in Ni^{II}H$_{-3}$L to the similar values of free L. We interpret that the third deprotonation occurs at the macrocyclic amine and that the resulting stronger N$_4$ ligand field weakens the axial coordination of the pyridine N-oxide.

Trivalent Copper and Nickel Ions. Electrochemical or chemical oxidation of M(II)–macrocyclic oxo tetraamine complexes in aqueous solutions results in the M(III) complexes. The copper(II) complexes lose their ESR signals when oxidized, going from a paramagnetic d^9 system to a low-spin diamagnetic d^8 system. Conversely, diamagnetic (low-spin) d^8 nickel(II)–dioxo tetraamine complexes have no ESR signal until oxidized, giving paramagnetic, low-spin d^7 complexes. The g values ($g_\parallel$ = ca. 2.20, $g_\perp$ = ca. 2.02) for the nickel(III) are characteristic of tetragonally distorted complexes with one unpaired electron in the d$_{z^2}$ orbital. These ESR spectra obtained at liquid-nitrogen temperature are similar to those for many of the previously reported Ni(III)–macrocyclic tetraamine complexes.[25,26]

(23) The formation constant K_{CuL} for 6 could not be determined by the pH-metric titration due to overly strong complexation.
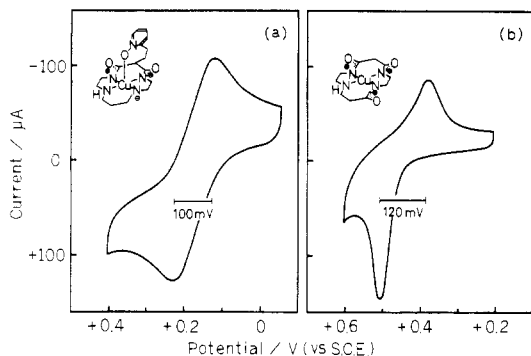(24) Kimura, E., unpublished data.

Figure 5. Cyclic voltammograms of $Cu^{II}H_{-3}L$ with $L = 11$ (a) and with $L = 12$ (b) in aqueous solution at a glassy-carbon electrode. In both cases $[CuH_{-3}L] = 2 \times 10^{-3}$ M in 0.5 M Na_2SO_4 and scan rate $= 100$ mV s^{-1}.

The ultraviolet–visible spectra of the majority of the present M(III) complexes are similar to those of unsubstituted dioxo complexes and peptide complexes, showing the intense charge-transfer absorptions at 380–400 nm for Cu and 340–360 nm for Ni. However, the electrochemical or chemical (with $Ir^{IV}Cl_6^{2-}$ or $(NH_4)_2S_2O_8$) oxidation of Cu(II) and Ni(II) complexes containing pyridine N-oxide or trioxo groups failed to give rise to such charge-transfer absorptions, although other evidence such as ESR spectra, magnetic susceptibility, or voltammograms (Figure 5) points to the formation of 1e-oxidized products.

The overall oxidation behavior of the macrocyclic M(II) complexes measures the thermodynamic stabilization of M(III) relative to M(II) and is a composite function of macrocyclic ring size, number of amide functions, type of appended substituents, and coordination number. With a broad family of complexes such as those described here, the observed pattern of behavior can be meaningfully related to other physical and chemical properties of these complexes. In general, the redox potentials $E°$ for the $Cu^{III,II}$–macrocycle complexes are highly dependent upon the natue of the ligands. On the other hand, the values of $E°$ for the $Ni^{III,II}$ complexes are much less sensitive to changes in the nature of the ligands.

Variation of Oxidation Properties with Structural Parameters. Effects of Macrocyclic Ring Size on $E°$. In a progression to larger macrocyclic rings (from 13- to 15-membered) containing common dioxo tetraamine functions (**1**, **8**, **17**), the low-spin d^8 Ni(II) → d^7 Ni(III) process is seen to occur with greater ease, while the d^9 Cu(II) → low-spin d^8 Cu(III) electrode reaction occurs with more difficulty, although the changes of $E°$ are not so remarkable. The macrocyclic ring size fitness of **1** over **8** and **17** to Ni(II) (compare d–d absorption values in Table II) would make the transition from Ni(II) to Ni(III) in the complex of **1** the most unfavorable. On the other hand, the easier oxidation of Cu(II) to Cu(III) in **1** would arise from the facile contraction of Cu(II) to Cu(III) in the narrowest 13-membered ring for Cu(II) (compare λ_{max} values of **1**, **8**, and **17** in Table II). Shorter metal–nitrogen bonds for Ni(II) (average 1.85 Å) compared to those for Cu(II) (1.93 Å) are well-known in square-planar peptide complexes.[13]

Effect of Imide Anion Coordination on $E°$. If one stays within the same chelated ligand framework and ring size, a noticeable effect is seen by the presence of various numbers of imide anions. The deprotonated peptide nitrogen is a strong in-plane donor and is a stronger σ donor than amine. Em-

(25) Lovecchio, F. V.; Gore, E. S.; Busch, D. H. *J. Am. Chem. Soc.* **1974**, *96*, 3109.

(26) Zeigerson, E.; Ginzburg, G.; Schwartz, N.; Luz, Z.; Meyerstein, D. *J. Chem. Soc., Chem. Commun.* **1979**, 241.

Table III. Dependence of $E°$ for $Cu^{III,II}$-**8** upon Solvent Composition and Temperature

solvent	temp, °C	$E°$, V (vs. SCE)[a]
water	25	0.693
22.5% 2-propanol	25	0.685
45.0% 2-propanol	25	0.678
75.0% 2-propanol	25	0.672
50.0% acetonitrile	25	0.652
50.0% acetone	25	0.653
water	15	0.688[b]
water	25	0.680[b]
water	35	0.673[b]

[a] $I = 0.1$ M $(NaClO_4)$ unless otherwise specified. [b] In 0.1 M Na_2SO_4.

pirically, replacement of an amine by a deprotonated amide lowers the $E°$ value by 0.15 V in peptide–Cu(II) complexes.[13] Hence, the higher the number of imide functions, the more stable is the Cu(III) state. To test whether this trend extends to macrocyclic tetraamines, we have progressively incorporated amide functions into the 14-membered tetraamines. The singly deprotonated monooxo **7**, the doubly deprotonated dioxo **8**, and the triply deprotonated trioxo **12** complexes with Cu(II) gave quasi-reversible cyclic voltammograms at $E°$ values of 0.86, 0.64, and 0.43 V (vs. SCE), respectively. It is thus concluded that the replacement of an amine group by imide anions in the macrocyclic tetraamines stabilizes the Cu(III) state as additively as in peptides.[13] It is of interest to recall that quadruply deprotonated tetraoxocyclam **21**, although it is not strictly homologous to our oxocyclam structures, has an $E°$ value of 0.23 V (vs. SCE),[22] which is 0.20 V lower than that of our trioxocyclam **12** and stays in the same line of additivity.

With nickel complexes of peptides, the stabilization by the imide anions also occurs, although the magnitude of the effect (0.02–0.06 V) is much smaller than with the copper complexes.[14] This is also true with 15-membered macrocycles; cf. **16** vs. **17**. However, the opposite trend is seen with 14-membered ligands (**5** vs. **8** in Table II). We ascribe this to unexpectedly low $E°$ values (0.50 V) for the oxo-free **5** and **6** due to the strong axial interaction of Ni(III) with SO_4^{2-} that was added for supporting electrolyte.[17] The use of the more weakly coordinating ligand ClO_4^- (0.1 M) in place of SO_4^{2-} (0.5 M) as a supporting electrolyte was found to raise the $E°$ value of Ni-**5** to 0.68 V. On the other hand, in the greater tetragonal distortion of the dioxo system **8** Ni(III) would not expect such strong axial interaction of sulfate. The facile axial coordination of an intramolecular N donor to Ni(III) is also seen with the oxo-free system **6**, but not with dioxo **10** (see the next paragraph). For the sake of comparison with previously reported unsaturated system,[25] we have measured $E°$ values for **22**

22   23
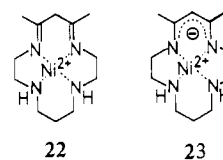
(=0.83 V vs. SCE at pH 4–5) and for **23** (=0.40 V vs. SCE at pH 9–10) under the present conditions containing 0.5 M Na_2SO_4. It is seen that the monoanionic Ni complex **23** has easier access to Ni(III) than our dianionic series.

Effect of Axial Coordination of Water. Changes in axial coordination of water may be expected upon oxidation of M(II)–macrocyclic N_4 complexes. Since those complexes containing metal ions with low-spin d^8 electronic configurations would have little or no axial coordination, a loss of two (ideally) axial water molecules for the oxidation of Cu(II) (eq 2) and

$$Cu^{II}(H_{-2}L)(H_2O)_2 \overset{-e^-}{\rightleftharpoons} Cu^{III}(H_{-2}L) + 2H_2O \qquad (2)$$
$$\quad\ d^9 \qquad\qquad\qquad\ \text{low-spin } d^8$$

$$Ni^{II}(H_{-2}L) + 2H_2O \overset{-e^-}{\rightleftharpoons} Ni^{III}(H_{-2}L)(H_2O)_2$$
$$\qquad\qquad\qquad\qquad\qquad\qquad\qquad (3)$$

$$Ni^{II}L + 2H_2O \overset{-e^-}{\rightleftharpoons} Ni^{III}L(H_2O)_2$$
$$\text{low-} \qquad\qquad\quad \text{low-spin } d^7$$
$$\text{spin}$$
$$d^8$$
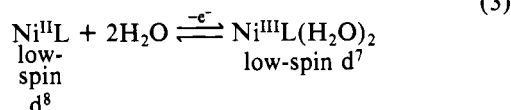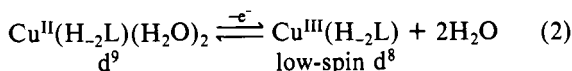
a gain of two water molecules for the oxidation of Ni(II) (eq 3) are reasonably assumed. To test the validity of eq 2 and 3, we measured E° values vs. SCE (25 °C) as a function of solvent composition. From eq 2, it is predicted that increasing the percentage of a nonaqueus solvent with poor solvating ability in a mixture with water should drive E° downward for the copper(II,III) couple. Table III gives the apparent E° value (ignoring problems with liquid-junction potential) for the Cu(H$_{-2}$L) couple for L = **8** in acetonitrile, acetone, and 2-propanol. The qualitative behavior in Table III suggests our prediction to be true, although the extent of solvent dependence is much less than with the reported Cu–peptide complexes.[27] Unfortunately, eq 3 could not be tested, since Ni(II)–dioxocyclam and –cyclam complexes failed to give reversible cyclic voltammograms in mixed solvents. The temperature dependences of E° for Cu^{II,III} couples of dioxocyclam **8** (648 mV at 15 °C, 643 mV at 25 °C, and 638 mV at 35 °C at [Na$_2$-SO$_4$] = 0.1 M) and for Ni^{II,III} complexes of oxo-free **5** (479 mV at 15 °C, 485 mV at 25 °C, and 491 mV at 35 °C at [Na$_2$SO$_4$] = 0.4 M and pH 3.0) are in support of eq 2 and 3.

Effect of Appended Substituent on E°. The phenyl and pyridyl substituents have virtually no effect on the electrode potentials for Cu(II) complexes of 13–15-membered dioxo tetraamines. This is in contrast to the alkyl substituent effect to stabilize the Cu(III) state with peptide complexes.[13] For instance, a benzyl substituent lowers the E° value 40 mV. This is explained as a combination of electron-donor ability and a steric interference of axial solvation, which is substantial for the d^9 Cu(II) complexes, but not for the d^8 Cu(III).[13] Linear peptide complexes of Cu(II) with more axial solvation would be more subject to such effects than the tetragonal macrocyclic tetraamine complexes.

The aromatic substituents have a negative effect on the stability of Ni(III) complexes of 13- and 14-membered dioxo tetraamines. The increase in the value of E° for **2** and **9** may be attributed to the interference of axial solvation of d^7 Ni(III) complexes with the aromatic side-chain group. When the aromatic substituents (such as benzyl and phenethyl) are on the oxo-free homologue, the values of E° (=0.50 V) do not differ from that for the unsubstituted **5** complex. As suggested earlier,[25] the strong axial interaction of SO$_4{}^{2-}$ with the Ni(III) complex would nullify the anticipated effect of the aromatic groups.

With the chemically oxidized product of pyridyl-tailing oxo-free complex of **6** with nickel, the ESR spectrum at liquid-N$_2$ temperature (Figure 6) shows axial symmetry, with $g_\perp > g_\parallel$. Further, $g_\parallel$ is split into three lines with intensity ratios of 1:1:1. This observation is consistent with the existence of a low-spin, d^7, five-coordinate Ni^{III} complex, in which the pyridyl N is axially coordinated. On the other hand, the absence of axially coordinated pyridyl N is indicated for the dioxo-homologue complex of **10** by the ESR spectrum showing no splitting of $g_\parallel$, although the relative magnitude of $g_\perp$ compared to that of $g_\parallel$ indicates a certain tetragonal geometry (with possible water coordination). These facts are compatible
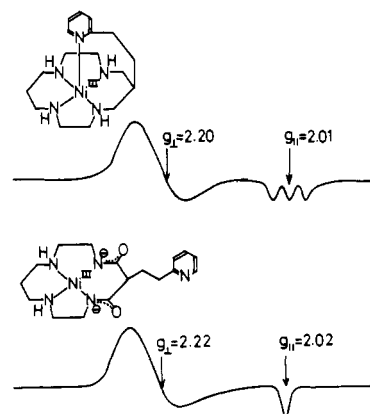
(27) Youngblood, M. P.; Margerum, D. W. *Inorg. Chem.* **1980**, *19*, 3068.

Figure 6. X-Band ESR spectra of Ni^{III}–**6** and Ni^{III}–doubly deprotonated **10** at 77 K.

with an observation by Busch et al.[25] that oxidation of neutral and dianionic macrocyclic tetraamine–Ni(II) complexes produces six-coordinate and square-planar Ni(III) species in acetonitrile, respectively.

The pyridine N-oxide substituent exerts the most dramatic effect on the stability of M(III). In particular, the E° values of the copper complexes are lower than those of any of the reported copper peptide complexes.[13] The reversible cyclic voltammograms were obtained only at high pH, where the M(II) complexes were triply deprotonated and formulated as MH$_{-3}$L (or MH$_{-2}$L(OH)). At lower pH, where the complexes are ordinary deprotonated species MH$_{-2}$L, the voltammograms are all irreversible. Of the common pyridine N-oxide macrocyclic complexes of copper, the ring size effect contributes more to the lower E° value for the 13-membered derivative **4** than for 14-membered **11**. The effect of imide anion coordination accounts for the lower E° value for the trioxocyclam derivative **15** than for dioxocyclam **11**. The ring size effect also accounts for the lower E° value for nickel complexes of 14-membered **11** than of 13-membered **4**.

As anticipated from the low E° values of 0.04–0.2 V, the copper(II) complexes of the pyridine N-oxide substituted macrocyclic **4**, **11**, and **15** in alkaline solutions are air oxidized, which is indicated by the color change from violet to green. The same color change is observed by electrochemical or chemical (e.g. (NH$_4$)$_2$S$_2$O$_8$) oxidation. However, thus formed Cu(III) species are very unstable and undergo further degradation to unidentified species. At present we have no evidence for the formation of O$_2$ adducts with these Cu(II) complexes. In our earlier experiment,[5] Ni(II) complexes of macrocyclic dioxo pentaamines possessing 0.24 V for Ni^{II,III} couples undergo smooth air oxidation, yielding 1:1 O$_2$ adducts.

It is difficult to see that the electron donor effect of the axial pyridine N-oxide ligand is the sole factor for stabilization of the trivalent copper and nickel complexes of macrocyclic tetraamines. Rather, the oxidized complexes may be in resonance with M(II) stabilized cation radicals of the pyridine N-oxide. This notion is partially supported by the ESR measurement of the (NH$_4$)$_2$S$_2$O$_8$-oxidized product of the Ni–**11** complex, which fails to show a spectrum characteristic of Ni(III) macrocyclic complexes but offered a new signal assignable to a nitrogen- or carbon-centered radical complex of Ni(II) ($g = 2.002$).

Conclusions

The copper(II) and nickel(II) macrocyclic tetraamine complex formulas and structures in aqueous solutions vary with the ring size, number of amide functions, and appended substituents. The triply deprotonated amide-containing N$_4$ ligands yield more stringently square-planar complexes with Cu(II) than any other ligands. The tetragonal distortion of dioxo tetraamine macrocyclic complexes is greater than that of linear

peptide complexes, preventing the axial interaction of the appended pyridyl N or solvents. On the other hand, the axial interaction of side-arm pyridine *N*-oxide is strongly indicated.

The $E°$ values of copper(II,III) couples are more subject to ligand structural effects than those of nickel(II,III) complexes. The $E°$ values successively diminish as the number of imide anions increases. The side-arm substituents do not significantly affect the $E°$ values. The greater tetragonal distortion with dioxocyclam complexes with respect to oxo-free cyclam complexes is evidenced by the fact that the pyridine N remains uncoordinated with Ni(III) for the former while it binds with Ni(III) for the latter.

Cu(III) was once proposed[28] to be part of the active site of galactose oxidase, although this was later questioned.[29] Recently Cu(III) has been postulated to be a mild oxidizing species in the oxidation of benzyl groups with Cu(II)–per-

oxydisulfate complexes.[30] Ni(III) is also postulated to be involved in hydrogenase activities.[31] Our study shows macrocyclic oxo polyamines to be a suitable model for biological redox reactions and other metal-catalyzed reactions.

Registry No. **1**, 71248-02-7; **2**, 92456-43-4; **3**, 92456-44-5; **4**, 92456-45-6; **5**, 295-37-4; **6**, 92456-46-7; **7**, 85828-26-8; **8**, 63972-19-0; **9**, 92456-47-8; **10**, 92456-48-9; **11**, 92456-49-0; **12**, 85828-27-9; **13**, 92456-50-3; **14**, 92456-51-4; **15**, 92456-52-5; **16**, 15439-16-4; **17**, 71248-03-8; **18**, 92456-53-6; **19**, 92456-54-7; **20**, 637-84-3; **21**, 92456-55-8; CH_2=CHCO$_2$Me, 96-33-3; diethyl (2-(2-pyridyl)-ethyl)malonate, 84199-92-8; 3,7-diazanonane-1,9-diamine, 4741-99-5; ethylenediamine, 107-15-3; 1,9-diamino-5-(2-(2-pyridyl)ethyl)-3,7-diazanonane-4,6-dione, 92456-56-9.

Supplementary Material Available: Calculation procedure for metal complex formation constants for (pyridylethyl)dioxo tetraamines and trioxocyclam (3 pages). Ordering information is given on any current masthead page.

(28) Hamilton, G. A.; Adolf, P. K.; Jersey, J.; Dubois, G. C.; Dyrkacz, G. R.; Libbiy, R. D. *J. Am. Chem. Soc.* **1978**, *100*, 1899.
(29) Winkler, M. E.; Bereman, R. D. *J. Am. Chem. Soc.* **1980**, *102*, 6244.

(30) Bhatt, M. V.; Perumal, P. T. *Tetrahedron Lett.* **1981**, *22*, 2605.
(31) Kojima, N.; Fox, J. A.; Hansinger, R. P.; Daniels, L.; Orme-Johnson, W. H.; Walsh, C. *Proc. Natl. Acad. Sci. U.S.A.* **1983**, *80*, 378.

Contribution from the Molecular Biology Institute and Department of Biological Chemistry,
School of Medicine, University of California, Los Angeles, California 90024

Zinc Ion in *Escherichia coli* DNA Polymerase: A Reinvestigation

DANIEL R. GRAHAM and DAVID S. SIGMAN*

The demonstration that the inhibition of *Escherichia coli* DNA polymerase I by 1,10-phenanthroline is due to the nicking of DNA by the 1,10-phenanthroline–copper complex of DNA rather than the coordination of tightly bound zinc ion has prompted the reexamination of the metal ion content of *Pol*I and the "Klenow fragment". Both proteins were purified to greater than 95% purity and dialyzed against a Chelex-treated 50 mM Tris-HCl buffer, pH 7.4. Although both enzymes had high specific activities for polymerization, they only contained 0.08–0.20 mol of Zn^{2+}/mol of enzyme upon analysis using atomic absorption spectrophotometry. The 3′-5′ exonuclease activity was also independent of zinc content. The rec A protein of *E. coli* likewise lacks zinc ions. Although RNA polymerase and the restriction endonuclease *Eco*RI contain zinc ion, our findings are not consistent with zinc ion serving a unique function in enzymes that use DNA as a substrate. 1,10-Phenanthroline and its metal complexes bind to DNA. Even if the DNA scission reaction of the 1,10-phenanthroline–copper complex is suppressed, this interaction provides another mechanism of inhibition of DNA and RNA polymerase that is not related to the presence of a tightly bound metal ion.

Introduction

The inhibition of DNA and RNA polymerases by 1,10-phenanthroline and the presence of zinc ion in those enzymes available in sufficient amounts for trace metal analyses led to the generalization that zinc ion is an essential component in all these enzymes.[1,2] The potential significance of this correlation has been emphasized by the demonstration in model reactions for prebiotic syntheses of RNA that zinc increased the yield of the 3′-5′ phosphodiester bonds at the expense of 2′-5′ phosphodiesters in the template-directed polymerization of imidazoyl-AMP by poly(U).[3-7] The zinc ion catalyzed phosphorylation of 1,10-phenanthroline-2-carbinol by ATP forming 1,10-phenanthroline-2-carbinol phosphate and ADP indicated the metal ion could play a more direct role in forming the internucleotide bond.[7] In this simple reaction, the metal

ion activates the carbinol for nucleophilic attack on the γ-phosphate of the ATP. By analogy, the zinc ion could coordinate the 3′-OH groups of the nascent RNA and DNA chains and enhance their nucleophilicity toward the α-phosphorus of an incoming nucleotide triphosphate.[8-10]

The first suggestion that 1,10-phenanthroline inhibition of polymerases did not reflect a central role of zinc ion was our demonstration that the kinetic effects observed with *Escherichia coli* DNA polymerase I[11] and DNA-dependent RNA polymerase and the RNA-dependent DNA polymerase of avian myeloblastosis virus[12] was due to the 2:1 1,10-phenanthroline–cuprous complex that can be formed from thiol and contaminating copper ion in assay mixtures. Subsequent studies have demonstrated that the inhibition of *E. coli* DNA

(1) Kornberb, A. "Supplement to DNA Replication"; W. H. Freeman: San Francisco, 1982; p 224.
(2) Mildvan, A. S.; Loeb, L. A. *CRC Crit. Rev. Biochem.* **1979**, *6*, 219–244.
(3) Lohrmann, R.; Bridson, P. K.; Orgel, L. E. *Science (Washington, D.C.)* **1980**, *208*, 1464–1465.
(4) Bridson, P. K.; Orgel, L. E. *J. Mol. Biol.* **1980**, *144*, 567–577.
(5) Lohrmann, R.; Orgel, L. E. *J. Mol. Biol.* **1980**, *142*, 555–567.
(6) van Roode, J. H. G.; Orgel, L. E. *J. Mol. Biol.* **1980**, *144*, 579–585.
(7) Inoue, T.; Orgel, L. E. *J. Am. Chem. Soc.* **1981**, *103*, 7666–7667.

(8) Sigman, D. S.; Wahl, G. M.; Creighton, D. J. *Biochemistry* **1972**, *11*, 2236–2242.
(9) Slater, J. P.; Tamir, I.; Loeb, L.; Mildvan, A. S. *J. Biol. Chem.* **1972**, *247*, 6784–6794.
(10) Springgate, C. F.; Mildvan, A. S.; Sbramson, R.; Engle, J. L.; Loeb, L. *J. Biol. Chem.* **1973**, *246*, 5987–5993.
(11) D'Aurora, V.; Stern, A. M. *Biochem. Biophys. Res. Commun.* **1977**, *78*, 170–176.
(12) D'Aurora, V.; Stern, A. M.; Sigman, D. S. *Biochem. Biophys. Res. Commun.* **1978**, *80*, 1025–1032.